Heliyon 10 (2024) e28642

Contents lists available at ScienceDirect

Heliyon

journal homepage: www.cell.com/heliyon

Research article

Supramolecular architecture of sodium heterocyclic dithiocarbamate salt: Insights from spectral analysis and bond valence sum characterization

Srinivasan N [a,b], S. Thirumaran [b,*]

[a] Department of Chemistry, Saveetha School of Engineering, Saveetha Institute of Medical And Technical Sciences (SIMATS), Saveetha Nagar, Thandalam, Chennai, 602105, Tamil Nadu, India
[b] Department of Chemistry, Annamalai University, Annamalainagar, 608 002, India

ARTICLE INFO

Keywords:
Heterocyclic dithiocarbamate
Coordination chemistry
Spectral analysis
Structural analysis
Hydrogen bonding
Bond valence sum analysis

ABSTRACT

The hydrated sodium salt of 1,2,3,4-tetrahydroquinolinedithiocarbamate (**1**) has been successfully synthesized and characterized using IR, NMR, and X-ray single crystal analysis. The υC–S and thioureide υC–N bands appeared at 1484 cm^{-1} and 968 cm^{-1}, respectively, in $Na(H2O)_3^+(thqdtc)^- \bullet H_2O$. The notable NCS_2 carbon signal emerged at 212 ppm, credited to unique nitrogen and sulfur-induced deshielding effects. Compound **1** crystallizes in the monoclinic system, P21/c space group, with dimensions a = 14.4297(4) Å, b = 6.1534(2) Å, c = 17.6701(4) Å, β = 108.7340(10)°, V = 1485.83(7) Å3, and Z = 4. The structure of 1 exhibits a supramolecular architecture through secondary interactions, such as weak intermolecular interactions that link the molecules into a linear polymeric chain. The incorporation of heterocyclic rings in the dithiocarbamate ligands leads to the formation of an intriguing supramolecular architecture, as confirmed by BVS analysis results. The BVS value of sodium does not agree well with the formal oxidation state due to the interactions of anions, cations, coordinated and uncoordinated water molecules.

1. Introduction

Dithiocarbamate anions find motivation in their utility across a diverse range of applications, spanning medicine, agriculture, organic synthesis, and even as synthetic precursors for metal sulfide nanoparticles [1–7]. Hydrated sodium ions play a crucial role in various biological functions of aquatic animals. Understanding hydrated sodium ions is challenging due to their biological mechanisms and the stabilization energy arising from the presence of multiple hydrates in these ions. Numerous clusters of hydrated sodium ions have been reported. The coordination geometry of these clusters is an intriguing feature, owing to sodium's coordination ability with water [8]. Many theoretical studies further support sodium atoms' hydrate coordination ability, leading to a variety of coordination environments for sodium ions. Alkali metal ions play a significant role in the biological functions of specific enzymes. The π–interactions of alkali metal cations are particularly interesting due to their aromatic residue sensing nature. R. Alan Howie and colleagues (2008) investigated a series of dithiocarbamate salts with hydrogen bonding functionality. The dtc ligand possesses a delocalized π–orbital system, allowing electron density transfer from nitrogen to sulfur [9].

* Corresponding author.
E-mail address: sthirumaran@yahoo.com (S. Thirumaran).

https://doi.org/10.1016/j.heliyon.2024.e28642
Received 24 July 2023; Received in revised form 19 March 2024; Accepted 21 March 2024
Available online 27 March 2024

Alkali metal dithiocarbamates exhibit significant pi interactions due to the presence of the NCS_2 moiety and water molecules. Among alkali metal dithiocarbamates, sodium, lithium, rubidium, and cesium metal dithiocarbamates have been reported in the literature. Alkali metal dithiocarbamates are water-soluble ionic compounds, resulting in the formation of many hydrated alkali metal dithiocarbamates. The coordination environment of alkali metals is influenced by water molecules. In this study, we synthesized a water-soluble hydrated sodium ionic compound with a dithiocarbamate moiety. To the best of our knowledge, few sodium salts of dithiocarbamates, such as $Na[S_2CN(CH_2CH_2OH)_2] \bullet 3H_2O$, $Na[S_2CN(CH_2CH_2OH)CH_2CH_2CH_3] \bullet 2H_2O$ [9], $Na_2[S_2CNH(CH_2)_2HNCS_2)] \bullet 6H_2O$ [10], and $Na_2[S_2CNCH_2C_6H_5CH_2CH_2N(CH_2C_6H_5)CS_2]$ [11], have been reported.

The influence of cations on the supramolecular aggregation patterns of dithiocarbamate anions, functionalized with hydrogen bonding capacity, stems from the prevalence of charge–assisted O–H/S interactions [9]. However, the literature lacks a polymeric structure of hydrated sodium ions among these structures. The sodium salt of 1,2,3,4–tetrahydroquinolinedithiocarbamate, hydrated sodium ions, leads to a polymeric structure without dithiocarbamate coordination. This structure possesses a unique structural motif compared to the reported hydrated sodium salts of dithiocarbamates. In this paper, we present sodium 1,2,3,4–tetrahydroquinolinedithiocarbamate tetrahydrate as an ideal subject for investigation, as sodium does not interact with the ligand's delocalized π–orbital system. The chemical composition of the present structure is illustrated in Scheme 1.

2. Experimental

2.1. Chemicals

Generally, 1,2,3,4-tetrahydroquinoline (Alfa Aesar), carbon disulfide (Merck), sodium hydroxide, and solvents (SD Fine) were commercially available high-grade materials and used as received.

2.2. Spectroscopy

IR spectra were recorded using a Thermo Nicolet Avatar 330 FT–IR spectrophotometer (range: 400–4000 cm–1) with KBr pellets. NMR spectra were recorded (in $CDCl_3$) on an AV–III 400 NMR spectrometer operating at 400 MHz.

2.3. X–ray crystallography

Details of the crystal data, data collection, and refinement parameters for $Na(H2O)_3^+(thqdtc)^- \bullet H_2O$ are summarized in Table 1. The intensity data were collected at ambient temperature (293(2) K) using a Bruker axs kappa apex2 CCD diffractometer with graphite monochromated MoKa radiation ($\lambda = 0.71073$ Å). The structure was solved using SIR–92 [12] and refined using a full matrix least square with SHELXL–97 [13]. All non-hydrogen atoms were refined anisotropically, and hydrogen atoms were refined isotropically. Bond distances and angles are provided in Table 2.

2.4. Synthesis of $Na(H_2O)_3^+(thqdtc)^- \bullet H_2O$

The sodium 1,2,3,4–tetrahydroquinoline-carbodithioate dihydrate was prepared using the following procedure [9,14]. A mixture of NaOH (50 mmol, 2.0 g) dissolved in a minimum quantity of water and 1,2,3,4–tetrahydroquinoline (50 mmol, 6.5 mL) was cooled to 5 °C in an ice bath. To this cold solution, CS_2 (50 mmol, 3.0 mL) was added in small portions while stirring. After 15 min, the entire mass solidified and was air-dried and recrystallized from an acetone–petroleum ether mixture (boiling range: 40–60 °C). Shining yellowish microcrystalline substance was collected and dried. Recrystallization of the yellowish microcrystalline $Na(H2O)_3^+(thqdtc)^- \bullet H_2O$ from a $CHCl_3$ solution yielded a pale yellow product. The pale yellow crystals were analyzed as $Na(H_2O)_3^+(thqdtc)^- \bullet H_2O$ (Scheme 2).

3. Results and discussion

In this paper, we aim to investigate the preparation and characterization using physical techniques such as IR, NMR, and single

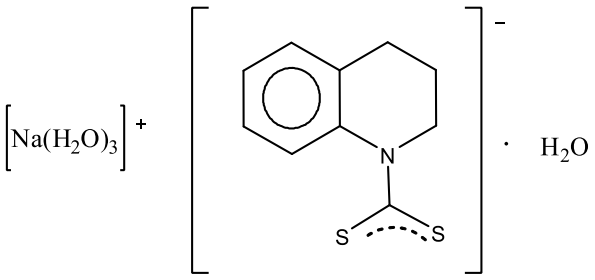

Scheme. 1. Chemical composition of $Na(H_2O)_3^+(thqdtc)^- \bullet H_2O$.

Table 1
Crystal data, data collection and refinement parameters for $Na(H_2O)_3^+(thqdtc)^- \bullet H_2O$.

Parameters	$Na(H_2O)_3^+(thqdtc)^- \bullet H_2O$
Empirical formula	$C_{10}H_{18}NO_4S_2Na$
FW	303.36
Crystal dimensions (mm)	0.26 × 0.22 × 0.20
Crystal system	Monoclinic
Space group	P21/c
a/Å	14.4297(4)
b/Å	6.1534(2)
c/Å	17.6701(4)
α/°	90.00
β/°	108.7340(10)
γ/°	90.00
U/Å^3	1485.83(7)
Z	4
DC/g cm^{-3}	1.356
μ/cm^{-1}	0.392
F(000)	640
λ/Å	MoK_α (0.71073)
θ Range/°	1.49–31.55
Index ranges	$-21 \le h \le 21$, $-9 \le k \le 9$, $-26 \le l \le 26$
Reflections collected	5404
Observed reflections $F_o > 4'O(F_o)$	4026
Weighting scheme	Calc. $W = 1/(\sigma^2(F_o^2) + (0.0750p)^2 + 0.1908p)$ where $p = (F_o^2 + 2F_c^2)/3$
Number of parameters refined	195
Final R, R_w(obs, data)	0.0403, 0.1171
GOOF	1.062

Table 2
Bond distances (Å) and angles (°) for $Na(H_2O)_3^+(thqdtc)^- \bullet H_2O$.

Bond distances (Å)		Bond angles (°)			
C8–N1	1.4735(18)	C5–C9–N1	117.50(13)	O3–Na1–O3^i	166.81(5)
C9–N1	1.4240(16)	C1–C9–N1	120.93(13)	O1–Na1–O3	95.00(5)
C10–N1	1.3463(17)	N1–C10–S2	118.96(9)	O2–Na1–O1	91.45(5)
C10–S2	1.7038(12)	N1–C10–S1	120.06(9)	O3–Na1–O1	102.69(5)
C10–S1	1.7164(12)	S2–C10–S1	120.98(8)	O1–Na1–O1^i	169.46(3)
O1–Na1	2.3612(13)	C10–N1–C9	125.48(10)	O3–Na1–O1^i	79.61(5)
O1^i–Na1	2.3871(13)	C10–N1–C8	122.11(12)	O2–Na1–O2^i	169.65(5)
O2–Na1	2.3357(13)	C9–N1–C8	112.21(12)	O2^i–Na1–Na1^i	47.75(3)
O2^i–Na1	2.4998(15)	Na1–O1–Na1^i	81.71(3)	O2–Na1–Na1^i	52.39(4)
O3–Na1	2.3577(15)	Na1–O2–Na1^i	79.86(4)	O3–Na1–Na1^i	141.41(5)
O3^i–Na1	2.3776(15)	Na1–O3–Na1^i	81.99(4)	O1^i–Na1–Na1^i	132.74(4)
Na1–Na1^i	3.1063(2)	O2–Na1–O3	115.63(6)	O3^i–Na1–Na1^i	48.73(4)
		O2–Na1–O1^i	96.18(5)	O1–Na1–Na1^i	48.78(3)
		O3–Na1–O1^i	80.54(5)	O2^i–Na1–Na1^i	118.26(4)
		O2–Na1–O3^i	77.05(5)	Na1^i–Na1–Na1^i	164.18(5)

Symmetry code: i = 2–x, 1/2+y, 1.5–z.

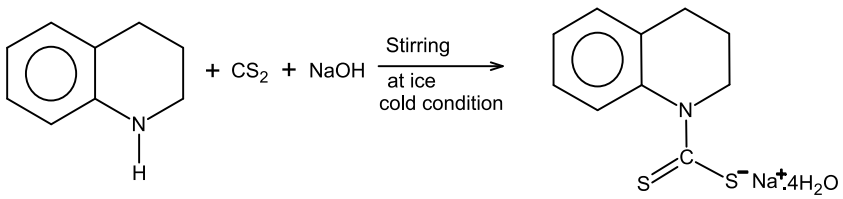

Scheme. 2. The preparation of $Na(H_2O)_3^+(thqdtc)^- \bullet H_2O$.

crystal analysis. Typically, dithiocarbamates exhibit high delocalization owing to the nature of pi electron movements from nitrogen to sulfur.

3.1. IR spectral studies

Dithiolate and dithiocarbamate ligands are very similar and peculiar; they exhibit high reactivity with alkali metals as well as other metals, forming compounds. In this study, the hydrated sodium salt of 1,2,3,4-tetrahydroquinolinedithiocarbamate (thqdtc) was formed due to the steric bulkiness of the dithiocarbamate ligand. Typically, the νC–N and νC–S stretching modes are significant absorption bands in dithiocarbamate complexes. The νC–N stretching mode has been utilized to gauge the contribution of the thioureide form (c) to the dithiocarbamate structure (Scheme 3).

The energy of the thioureide νC–N band falls in between the stretching frequencies associated with typical singly and doubly bonded carbon and nitrogen (Fig. 1). This can be best explained as the vibration of the polar C═N band [15,16]. A νC–N band of moderate intensity, around 1450 cm^{-1}, has been previously observed [17]. In $Na(H_2O)_3^+(thqdtc)^- \bullet H_2O$, the thioureide νC–N band at 1484 cm^{-1}. Water bands are observed in the 3422–3250 cm^{-1} region in Na(thqdtc) • $4H_2O$. The νC–S bands appear at 968 cm^{-1} in $Na(H_2O)_3^+(thqdtc)^- \bullet H_2O$ [18]. The C═C Stretching, usually observed at 1641and1593 cm^{-1}. The CH and CH_2 stretching vibrations were assigned at 3008 cm^{-1} and 2936 cm^{-1}, respectively.

3.2. NMR spectral studies

Free 1,2,3,4–tetrahydroquinoline exhibits signals at 3.29 and 6.46 ppm for protons at C-2 and C-8, respectively. The ^1H NMR spectrum of $Na(H_2O)_3^+(thqdtc)^- \bullet H_2O$ (Fig. 2) reveals that protons at C-2 and C-8 undergo strong deshielding, resulting in signals at 4.3 and 7.2 ppm, respectively. The observed deshielding of the protons at C-2 and C-8 in $Na(H_2O)_3^+(thqdtc)^- \bullet H_2O$ is attributed to the release of electrons from the NR_2 groups, causing a high electron density towards the sulfur via the thioureide π–system [19]. Other proton signals remain relatively unaffected in $Na(H_2O)_3^+(thqdtc)^- \bullet H_2O$ due to their distance from the thioureide π–system. A quintet observed around 2.10 and a triplet observed around 2.75 ppm are attributed to the protons at C-3 and C-4, respectively. A multiplet observed in the region of 7.12–7.22 ppm is assigned to the protons at C-5, C-6, and C-7 in thqdtc. Free 1,2,3,4–tetrahydroquinoline displays a signal at 41.9 ppm due to the C-2 carbon. In the case of $Na(H_2O)_3^+(thqdtc)^- \bullet H_2O$, C-2 carbon is deshielded, resulting in signal at 52.7 ppm. The downfield shift of the C-2 carbon signal in the case of Na(thqdtc)•$4H_2O$ is due to a reduction in the electron density in their vicinity, contributing to a significant thioureide structure $N\delta^+ C\delta^-$ in the salt. In $Na(H_2O)_3^+(thqdtc)^- \bullet H_2O$, the aromatic carbons of thqdtc are observed in the region of 125.2–143.4 ppm. The important NCS_2 carbon signal is found at 212.6 ppm due to the deshielding effects of nitrogen and sulfur in the thqdtc ligand (Fig. 3). This result indicates that the dithiocarbamate anion is not coordinated with sodium metal.

3.3. Single crystal X–ray analysis of $Na(H_2O)_3^+(thqdtc)^- \bullet H_2O$

The single crystal X–ray structure of $Na(H_2O)_3^+(thqdtc)^- \bullet H_2O$ reveals four formula units per unit cell (Figure S1), and the [Na $(H_2O)_3^+$] units aggregate into linear polymeric chains (Fig. 4). Fig. 5 illustrates that one of the four water molecules in Na $(H_2O)_3^+(thqdtc)^- \bullet H_2O$ acts as a bridging unit between [$Na(H_2O)_3^+$] and thqdtc (O3–H3b … O1w–H1d … S1).

The Na^+ ion is coordinated by six water oxygen atoms at distances ranging from 2.3357(13) to 2.4998(15) Å, forming a distorted octahedron. The O–Na–O bond angles range from 74.31(5) to 169.65(6)%. No Na–S bonds are formed; instead, S1 and S2 accept four oxygen and two hydrogen bonds from the water molecules, respectively, with S···H distances in the range of 2.41(3)–2.70(3) Å and S···O distances from 3.2743(15) to 3.4423(18) Å (Table 3). The C10–S1 bond length is 1.7164(12) Å, and the C10–S2 bond length is 1.7038(12) Å, showing a slight difference.

The four S1···H–O hydrogen bonds are responsible for the lengthening of the C10–S1 bonds. It has been previously reported [20] that in the case of disodium 1,4–piperazinecarbodithioate hexahydrate, the C–S bond lengths are influenced by the number of hydrogen bonds accepted by the sulfur atoms. Since C10 is involved in three bonds [C10–N1, C10–S1, and C10–S2] with a partial double bond character, the bond angles around C10 are very close to 120°.

In contrast, the N atom is surrounded by one partial double bond [N1–C10] and two single bonds [N1–C8 and N1–C9]; thus, the C8–N1–C9 angle [112.21(12)%] is markedly smaller than the other two. This is a common feature of the dithiocarbamates [21,22], as well as dithiocarbamates with organic cations [23,24].

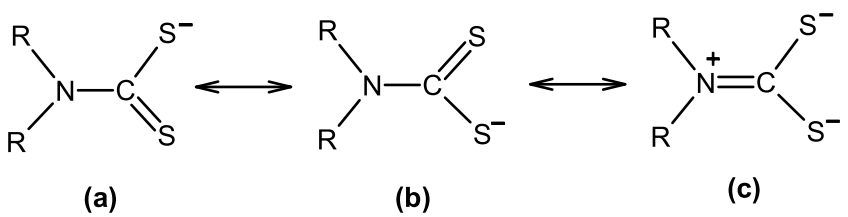

Scheme. 3. The resonance forms of NCS_2.

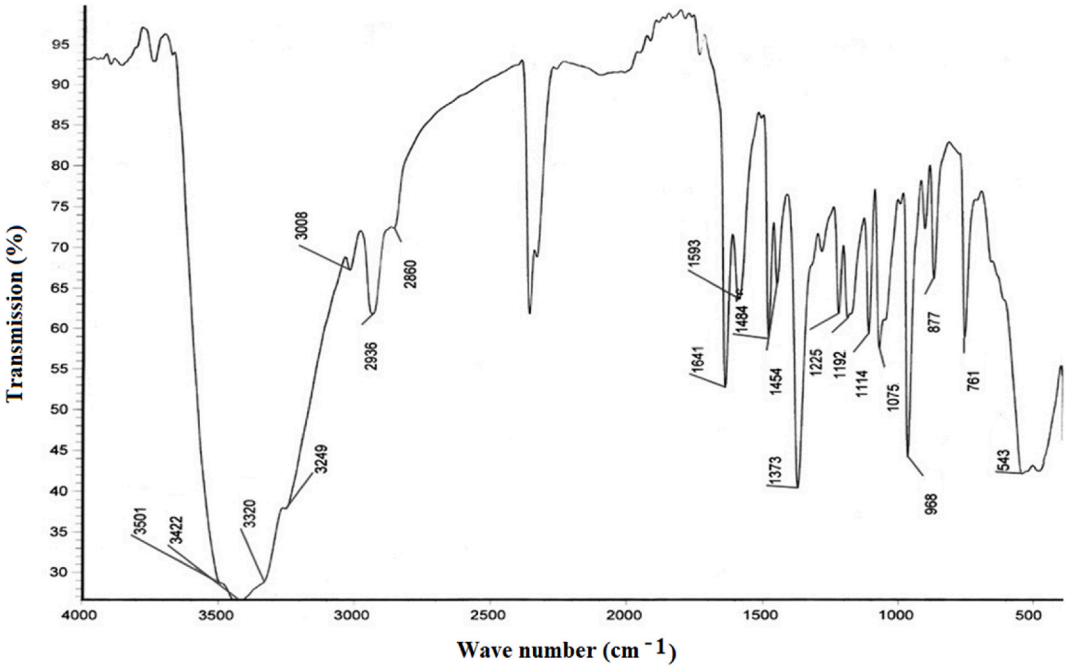

Fig. 1. IR spectrum of $Na(H_2O)_3^+(thqdtc)^- \bullet H_2O$.

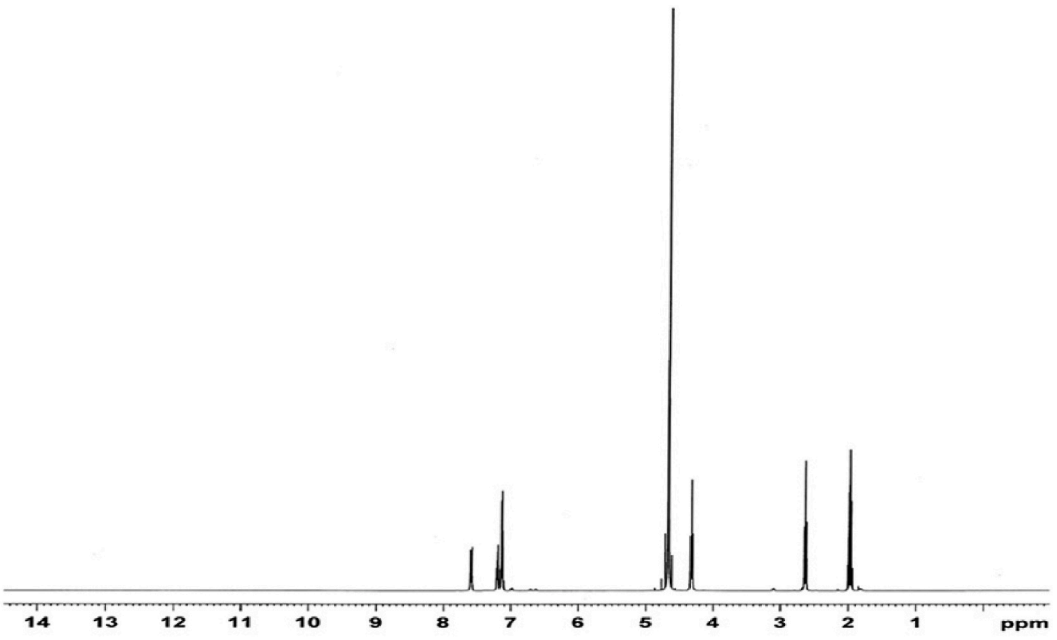

Fig. 2. ^1H NMR spectrum of $Na(H_2O)_3^+(thqdtc)^- \bullet H_2O$.

A helical-like grid architecture is formed by a $[Na(H_2O)_3^+]$ unit and another unit of $[Na(H_2O)_3^+]$ moieties, which are linear polymeric chains with a larger number of $[Na(H_2O)_3^+]$ moieties, as depicted in Figure S2. A net-like architecture (Figure S3) is also formed through the dtc organic ligand, water molecules, and $[Na(H_2O)_3^+]$ units. The dithiocarbamate reveals that the bulkiness of the pendant group in the dithiocarbamate part of the compound plays an important role in the construction of the supramolecular architecture through water O in $[Na(H_2O)_3^+]$/S interactions.

As anticipated, complex 1 features interesting intermolecular dtc–H(benzyl)/dtc–H(benzyl) and dtc–C(benzyl)/dtc–H(benzyl) secondary bonding, leading to the formation of a layer-like architecture (Figure S4). These dtc–H(H8B)/dtc–H(H8B) and dtc–C(C8)/

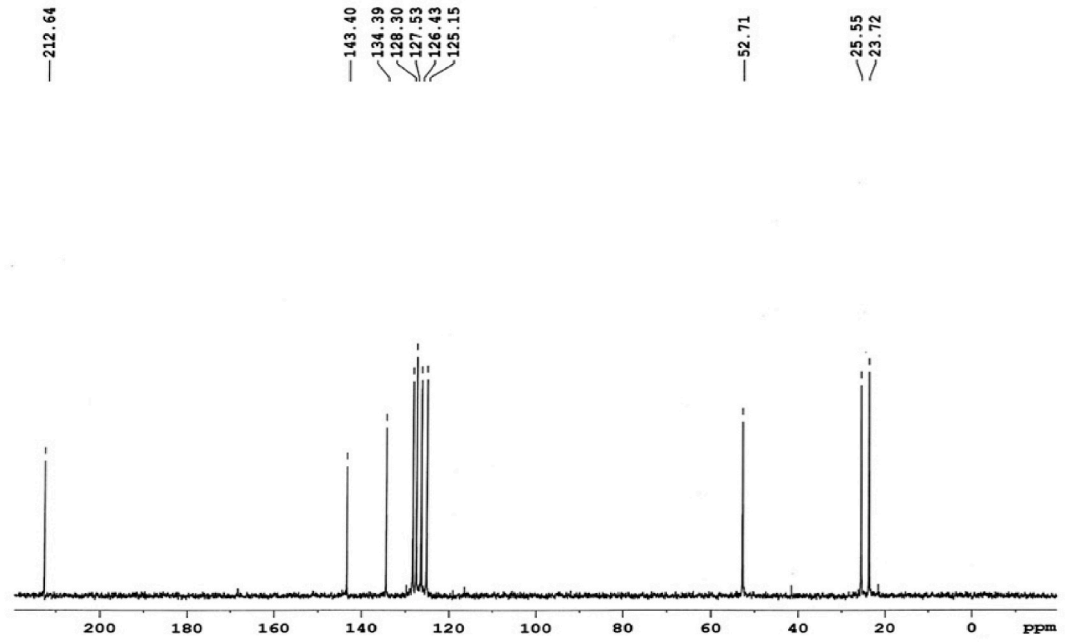

Fig. 3. ^{13}C NMR spectrum of $Na(H_2O)_3^+(thqdtc)^- \bullet H_2O$.

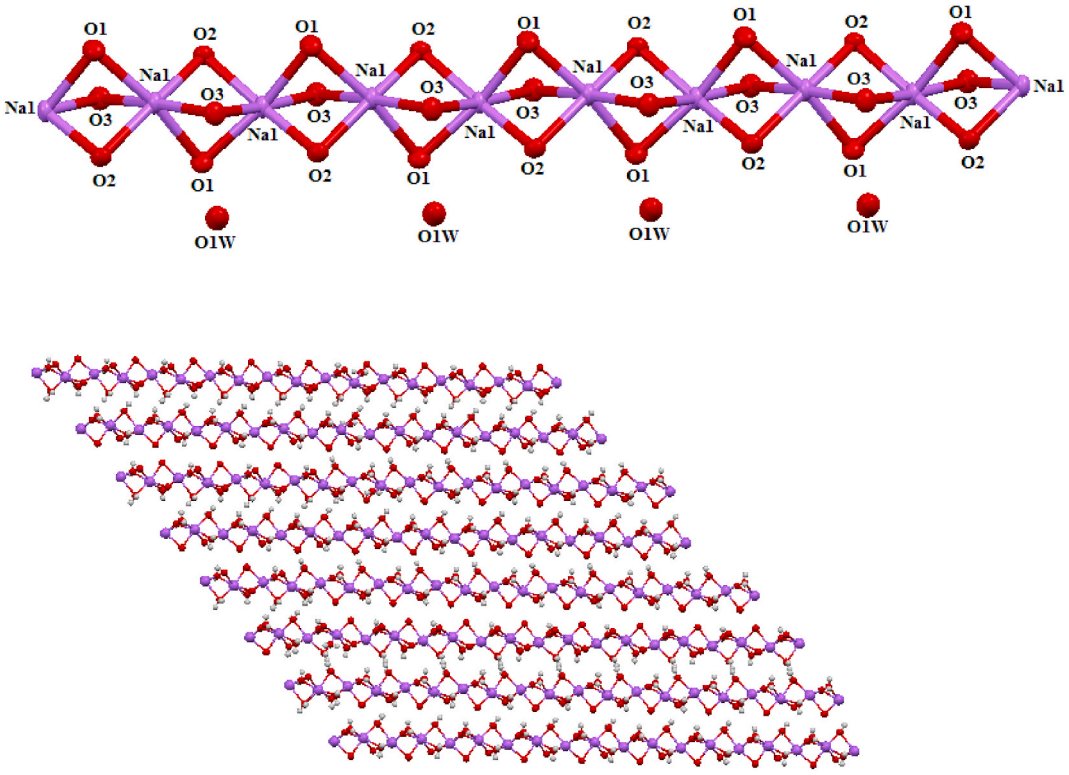

Fig. 4. Linear polymeric chain formed by $[Na(H_2O)_3^+]$ (symmetry code: i = 2–x, 1/2+y, 1.5–z).

dtc–H(H8B) contacts, with dimensions of 2.3717 (1) Å and 2.892(2) Å, respectively, are comparable to the sum of the van der Waals radii of the respective elements (rvdw (H) = 1.2 Å and rvdw (C) = 1.70). In this structure, there are four O–H/O hydrogen bonding contacts and O–H/S interactions that exclusively serve to stabilize the layers.

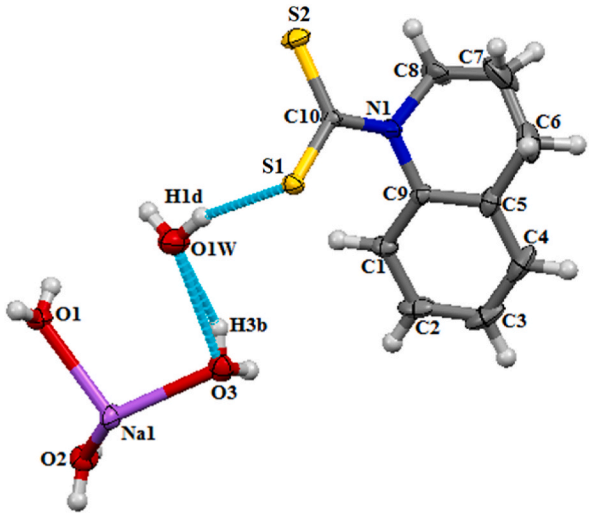

Fig. 5. ORTEP diagram of $Na(H_2O)_3^+(thqdtc)^- \bullet H_2O$.

Table 3
Hydrogen–bonding geometric parameters for $Na(H_2O)_3^+(thqdtc)^- \bullet H_2O$ [(Å), (%)].

H–bond	D···H	H···A	D···A	D–H···A
O1–H1A···S1	0.84(3)	2.45(3)	3.2793(14)	168(2)
O1–H1B···S1	0.71(3)	2.70(3)	3.3137(12)	146(3)
O1W–H1C···S1	0.82(4)	2.65(4)	3.4423(18)	162(4)
O1W–H1D···S1	0.85(3)	2.59(3)	3.3959(17)	159(3)
O2–H2A···O1W	0.85(3)	2.23(3)	2.974(3)	147(3)
O2–H2B···S2	0.89(3)	2.41(3)	3.2743(15)	165(3)
O3–H3A···S2	0.82(3)	2.58(3)	3.2954(17)	147(3)
O3–H3B···O1W	0.77(3)	2.22(3)	2.865(2)	142(2)

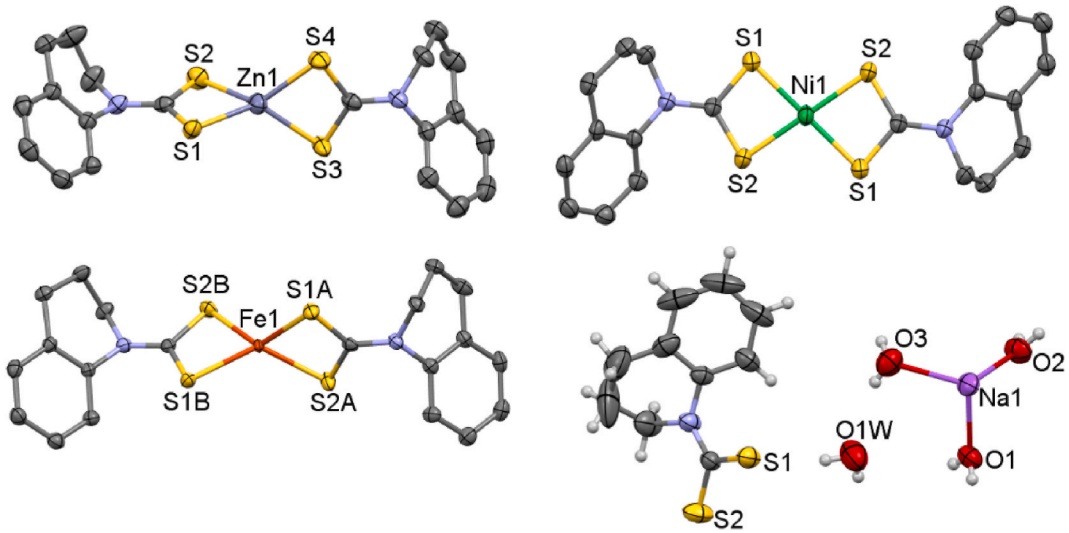

Fig. 6. Delineating the structural geometry of tetrahydroquinoline dithiocarbamate (thqdtc) with various metals.

Tetrahydroquinoline dithiocarbamate complexes would generally involve the coordination of the dithiocarbamate ligands to the metal ions (zinc, nickel, or iron, see Fig. 6) [25–27]. The dithiocarbamate ligands coordinate in a bidentate manner through the sulfur atoms, forming chelate complexes. The exact coordination geometry, bonding angles, and other structural features can vary based on factors such as the specific metal ion (transition metals), oxidation state (+2), ligand environment, and experimental conditions. Zinc

and iron typically engage with dithiocarbamate, resulting in tetrahedral or square planar geometries, aligning with their distinctive (d^{10}, d^6) electronic configurations. Interestingly, both zinc and iron exhibit a preference for the tetrahedral geometry. Conversely, nickel, with its d^8 electronic configuration, predominantly adopts the square planar geometry, presenting a noteworthy structural variation in dithiocarbamate complexes.

3.4. Bond valence sum

Bond valence sum analysis is an important tool to confirm the oxidation states of metals in metal complexes, ionic liquids, or salts. It is also helpful in checking the quality or precision of crystallographic data. In some cases, the R value is low or high depending on the accuracy of crystal data; this includes anisotropic thermal parameters and any disordered molecules. The calculated BVS value should agree with the corresponding oxidation state of the molecules, reflecting the accuracy of the crystal data. If the calculated BVS value does not agree with the oxidation state, it indicates that the oxidation state is wrongly identified, the metal may have been chosen incorrectly, or there may be issues with other interactions or imprecise crystal data [28].

The provided tools calculate the oxidation state of metals in metal complexes using the following equations: $Zj = \sum Sij$, $Sij = \exp[(R0- Rij)/b)]$, where Zj represents the oxidation state, Sij is the sum of individual bond valences, and b is a constant (0.37). Additionally, the EXPO2014 software [29] is employed to determine bond valence sums for the obtained ionic liquids, yielding details such as atoms, bond distances, and bond valence values, presented in a Table 4.

In general, the oxidation state of sodium metal is considered as 1. However, the BVS analysis yielded values of 1.251 and 1.0670 for sodium metal, which do not align well with its formal oxidation state. These results suggest a charge imbalance in sodium metals likely caused by the influence of coordinated and uncoordinated water molecules, as well as the dithiocarbamate anion. Notably, the two BVS values diverge due to the precision of the data.

4. Conclusions

The synthesis of the hydrated sodium salt of 1,2,3,4–tetrahydroquinolinedithiocarbamate was achieved through a reaction involving 1,2,3,4–tetrahydroquinoline and carbon disulfide with sodium hydroxide. Comprehensive characterization was conducted utilizing IR, NMR, and single crystal X–ray structural analysis. Significant findings from this study indicate that no coordination bond forms between the dithiocarbamate ligand and sodium metal. This is attributed to the pronounced repulsion between sulfur and nitrogen in dithiocarbamate. The structural analysis reveals the composition comprising one hydrated sodium anion, one dithiocarbamate cation, and an uncoordinated water molecule. Interestingly, the $[Na(H_2O)_3^+]$ cation was found to construct a supramolecular architecture, influenced by the bulkiness of the tetrahydrouinoline group within the dithiocarbamate segment of the compound. This structural aspect plays a pivotal role in shaping the supramolecular architecture.

Furthermore, bond valence sum analysis provided additional support for the formation of this distinctive supramolecular architecture, emphasizing the imbalance in the formal oxidation state of sodium. These results underscore the intriguing nature of the synthesized compound and its potential for various applications and further research.

Data availability

Crystallographic data have been deposited (CCDC 2280947) with the Cambridge Crystallographic Centre. A copy of the data can be obtained free of charge, and applications can be directed to CCDC, 12 Union Road, Cambridge CBZ 1FZ UK.

CRediT authorship contribution statement

Srinivasan N: Writing – original draft, Investigation, Conceptualization. **S. Thirumaran:** Writing – review & editing, Supervision, Conceptualization.

Table 4
Bond Valence sum of Na in $Na(H_2O)_3^+(thqdtc)^- \bullet H_2O$.

Bond	Bond distance(Å)	EXPO2014 software [29]	Sij = exp[(R0- Rij)/b)]
		BV(v.u.)	BV(v.u.) Using Sij [28]
Na–O1	2.387	0.206	0.1759
Na–O1	2.361	0.221	0.1887
Na–O2	2.336	0.237	0.2019
Na–O2	2.500	0.152	0.1296
Na–O3	2.358	0.223	0.1902
Na–O3	2.377	0.212	0.1807
BVS for the obtained ionic liquids		1.251	1.0670

Declaration of competing interest

The authors declare the following financial interests/personal relationships which may be considered as potential competing interests:S. Thirumaran reports was provided by Department of Chemistry, Annamalai University, Annamalainagar 608 002, India. N. Srinivasan reports a relationship with Department of Chemistry, Annamalai University, Annamalainagar 608 002, India. that includes:. N. Srinivasan If there are other authors, they declare that they have no known competing financial interests or personal relationships that could have appeared to influence the work reported in this paper.

Appendix A. Supplementary data

Supplementary data to this article can be found online at https://doi.org/10.1016/j.heliyon.2024.e28642.

References

[1] B. Cvek, Z. Dvorak, Targeting of nuclear factor-kappaB and proteasome by dithiocarbamate complexes with metals, Curr. Pharmaceut. Des. 13 (2007) 3155–3167, https://doi.org/10.2174/138161207782110390.

[2] H. Li, C.S. Lai, J. Wu, P.C. Ho, D. de Vos, E.R.T. Tiekink, Cytotoxicity, Qualitative Structure-Activity Relationship (QSAR), and anti-tumor activity of bismuth dithiocarbamate complexes, J. Inorg. Biochem. 101 (2007) 809–816, https://doi.org/10.1016/j.jinorgbio.2007.01.010.

[3] O.H.J. Szolar, Environmental and pharmaceutical analysis of dithiocarbamates, Anal. Chim. Acta 582 (2007) 191–200, https://doi.org/10.1016/j.aca.2006.09.022.

[4] R.S. Grainger, P. Innocenti, New applications of dithiocarbamates in organic synthesis, Heteroat. Chem. 18 (2007) 568–571, https://doi.org/10.1002/hc.20336.

[5] D. Fan, M. Afzaal, M.A. Malik, C.Q. Nguyen, P. O'Brien, P.J. Thomas, Using coordination chemistry to develop new routes to semiconductor and other materials, Coord. Chem. Rev. 251 (2007) 1878–1888, https://doi.org/10.1016/j.ccr.2007.03.021.

[6] M.S. Vickers, J. Cookson, P.D. Beer, P.T. Bishop, B. Thiebaut, Dithiocarbamate ligand stabilised gold nanoparticles, J. Mater. Chem. 16 (2006) 209–215, https://doi.org/10.1039/B509173J.

[7] Y.W. Koh, C.S. Lai, A.Y. Du, E.R.T. Tiekink, K.P. Loh, Growth of bismuth sulfide nanowire using bismuth trisxanthate single source precursors, Chem. Mater. 15 (2003) 4544–4554, https://doi.org/10.1021/cm021813k.

[8] P. Wang, R. Shi, Y. Su, L. Tang, X. Huang, J. Zhao, Hydrated sodium ion clusters $[Na^+(H_2O)_n$ (n = 1–6)]: an *ab initio* study on structures and non–covalent interaction, Front. Chem. 7 (2019) 624–634, https://doi.org/10.3389/fchem.2019.00624.

[9] R. Alan Howie, Geraldo M. de Lima, Daniele C. Menezes, James L. Wardell, Solange M.S. V. Wardell, David J. Youngce, Edward R.T. Tiekink, He influence of cation upon the supramolecular aggregation patterns of dithiocarbamate anions functionalised with hydrogen bonding capacity—the prevalence of charge-assisted O–H···S interactions, CrystEngComm 10 (2008) 1626–1637, https://doi.org/10.1039/B809730E.

[10] V. Vrable, S. Gergely, J. Lokaj, E. Kello, J. Garaj, Structure of disodium ethylenebisdithiocarbamate hexahydrate, Acta Crystallogr., Sect. C: Cryst. Struct. Commun. 43 (1987) 2293–2295, https://doi.org/10.1107/S0108270187088012.

[11] Reyna Reyes–Martınez, Herbert Hopfl, Carolina Godoy–Alcantar, Felipe Medrano, Hugo Tlahuext, Comparative analysis of M–O, M–S and cation–p(arene) interactions in the alkali metal (Na^+,K^+,Rb^+,Cs^+) bis–dithiocarbamate salts of N,N'–dibenzyl–1,2–ethylene-diamine, CrystEngComm 11 (2009) 2417–2424, https://doi.org/10.1039/B907160A.

[12] A. Altomare, M.C. Burla, M. Camalli, G. Cascavano, G. Giacovazzo, A. Guagliardi, G. Polidori, A new tool for crystal structure determination and refinement, J. Appl. Crystallogr. 27 (1994) 435, https://doi.org/10.1107/S002188989400021X.

[13] G.M. Sheldrick, SHELXL–97, Program for Crystal Structure Solution and Refinement, University of Gottingen, Gottingen, Germany, 1997.

[14] B.S. Garg, R.K. Garg, M.J. Reddy, Synthesis and spectral characterization of zinc(II), cadmium(II) and mercury(II) with tetrahydroquinoline and isoquinoline dithiocarbonates, Indian J. Chem. A. 32 (1993) 697–700. http://nopr.niscair.res.in/handle/123456789/43948.

[15] L. Ronconi, L. Giovagnini, C. Marzano, F.B. Effio, R. Graziani, G. Pilloni, D. Fregona, Gold dithiocarbamate Derivatives as potential Antineoplastic agents: design, spectroscopic properties, and in vitro antitumor activity, Inorg. Chem. 44 (2005) 1867–1881, https://doi.org/10.1021/ic048260v.

[16] R. Baggio, A. Frigerio, E.B. Halac, D. Vega, M. Perec, Anionic halide and isothiocyanate adducts of zinc and cadmium dithiocarbamates, J. Chem. Soc. Dalton Trans. (1992) 549–554, https://doi.org/10.1039/DT9920000549.

[17] G. Aravamudan, D.H. Brown, D. Venkappayya, Some metal complexes of morpholine-4-carbodithioate, J. Chem. Soc. A (1971) 2744, https://doi.org/10.1039/J19710002744.

[18] F. Bonati, R. Ugo, Tin(IV) dithiocarbamates and related compounds, J. Organomet. Chem. 10 (1967) 257–268, https://doi.org/10.1016/S0022-328X(00)93085-7.

[19] N. Srinivasan, S. Thirumaran, S. Ciattini, Effect of position of methyl substituent in piperidinedithiocarbamate on the ZnS4N chromophore: synthesis, spectral, valence-bond parameters and single crystal X-ray structural studies on bis(2-methylpiperidinecarbodithioato-S,S')-(pyridine)zinc(II) and bis(4-methylpiperidinecarbodithioato-S,S)(pyridine)zinc(II), J. Mol. Struct. 936 (2009) 234–238, https://doi.org/10.1016/j.molstruc.2009.08.001.

[20] J.P. Legros, D. Troy, J. Galy, Structure of disodium 1,4-piperazinedicarbodithioate hexahydrate, 2Na+.C6H8N2S42-.6H2O, Acta Crystallogr. C 40 (1984) 801–804, https://doi.org/10.1107/S0108270184005783.

[21] V. Vrabel, S. Gergely, J. Lokaj, E. Kello, J. Garg, Structure of disodium ethylenebisdithiocarbamate hexahydrate, Acta Crystallogr. C 43 (1987) 2293–2295, https://doi.org/10.1107/S0108270187088012.

[22] I. Ymen, C. Acta Crystallogr, Structure of sodium diisopropyldithiocarbamate pentahydrate, Na[C7H14NS2].5H2O 39 (1983) 874–877, https://doi.org/10.1107/S010827018300668X.

[23] R. Reyes–Martinez, H. Hopfl, C. Godoy–Alcantar, F. Medrano, H. Tlahuext, Comparative analysis of M–O, M–S and cation–π(arene) interactions in the alkali metal (Na+, K+, Rb+, Cs+) bis-dithiocarbamate salts of N,N′-dibenzyl-1,2-ethylenediamine, CrystEngComm 11 (2009) 2417–2424, https://doi.org/10.1039/B907160A.

[24] R. Alan Howie, G.M. de Lima, D.C. Menezes, J.L. Wardell, S.M.S.V. Wardell, D.J. Young, E.R.T. Tiekink, The influence of cation upon the supramolecular aggregation patterns of dithiocarbamate anions functionalised with hydrogen bonding capacity—the prevalence of charge-assisted O–H···S interactions, CrystEngComm 10 (2008) 1626–1637, https://doi.org/10.1039/B809730E.

[25] Narayanaswamy Srinivasan, Subbiah Thirumaran, Synthesis of ZnS nanoparticles from pyridine adducts of zinc(II) dithiocarbamates, Compt. Rendus Chem. 17 (2014) 964–970, https://doi.org/10.1016/j.crci.2013.10.009.

[26] P. Valarmathi, N. Srinivasan, S. Thirumaran, Synthesis and spectral studies of Ni(II) heterocyclic dithiocarbamates with S2PN chromophore: X-ray crystal structures of bis(1,2,3,4-tetrahydroquinolinecarbodithioato- S,S')nickel(II) and 1,2,3,4-tetrahydroquinolinecarbodithioato-S,S')(thiocyanato-N)(triphenylphosphine)nickel(II), J. Sulfur Chem. 32 (2011) 583, https://doi.org/10.1080/17415993.2011.628991.

[27] S. Saeed, R. Hussain, Ray J. Butcher, Growth of semiconducting iron sulfide thin films by chemical vapor deposition from air-stable single-source metal organic precursor for photovoltaic application, J. Coord. Chem. 67 (2014) 1693–1701, https://doi.org/10.1080/00958972.2014.918265.
[28] R.M. Wood, G.J. Palenik, Bond valence sums in coordination chemistry. Sodium−Oxygen complexes, Inorg. Chem. 38 (1999) 3926–3930, https://doi.org/10.1021/ic9903331.
[29] A. Altomare, C. Cuocci, C. Giacovazzo, A. Moliterni, R. Rizzi, N. Corriero, A. Falcicchio, EXPO2013: a kit of tools for phasing crystal structures from powder data, J. Appl. Crystallogr. 46 (2013) 1231–1235, https://doi.org/10.1107/S0021889813013113.